Changing dendritic excitability with A-type K+ channels

Jeffrey Bush
Neurosciences Graduate Program
University of California San Diego
La Jolla, CA 92093
jbush@salk.edu

Justin Kiggins
Neurosciences Graduate Program
University of California San Diego
La Jolla, CA 92093
jkiggins@ucsd.edu

Abstract

Spike timing dependent plasticity is a critical component of long term synaptic changes that seem to account for Hebbian-type learning and relies in many cases on backpropagating action potentials. However, it is unclear how variation in the morphology and conductance properties of the dendritic tree affect backpropagating action potential success. Recent evidence indicates that A-type K+ channel density can change with activity and has the potential to modulate the excitability of individual dendritic branches. In order to explore the possible interactions between morphology and A-type K+ channel density at dendritic branches, we implemented a compartmental model of CA1 dendrites with two branches and analyzed both the simulated neuron and the underlying travelling wave attractors. Our model indicates that modulation of A-type K+ channel density has the potential to significantly affect both the magnitude and relative timing of bAPs, especially for small diameter branches. This would provide a unique mechanism for cells to determine whether certain branches "qualify" for STDP.

1 Introduction

At the synapse, spike timing dependent plasticity (STDP) depends on the specific timing of excitatory post synaptic potentials (EPSPs) and back-propagating action potentials (bAP). However, the effectiveness of bAPs at invading the dendrites is not equal for all dendrites, as more distal dendrites in hippocampal CA1 pyramidal cells show decreased amplitude of bAPs and greater likelihood of failure at branch points [1], sending different patterns and amplitudes of bAPs down different branches of the dendritic tree. Such failures in bAPs could be due to a combination of morphology and dendritic excitability and computational modeling of bAPs indicates that A-type K+ channels can account for differences in the success of bAPs invading into distal dendrites [2]. These "failures" would mean the potential for different types of STDP varies along different branches of the dendritic tree. Since bAPs are modulated by dendritic A-type K+ channels, knocking out the Kv4.2 gene (and therefore A-type K+ channels) enhances LTP [3]. Further, Kv4.2 channel distribution can change based on activity, increasing dendritic excitability [4]. Recent work indicates that enriched environments result in stronger pairing of select daughter and parent dendrites due to down regulation of A-type K+ channels [5]. Thus, changes in activation of Kv4.2 along dendrites can change the potential for dendrites to acts as pathways for bAPs to reach selected synapses, modulating the potential for STDP.

Though prior computational modeling has addressed the relative contributions of dendritic morphology and A-type K+ channel density on the ability of bAPs to invade distal dendrites in CA1 [2], this work assumed that changes in A-type channel density changed relative to the distance from the soma and did not address whether differential changes in excitability at branch points could target bAPs. Here we use a simplified single branch model of a CA1 pyramidal cell dendrite to investigate the relative contributions of morphology and A-type K+

channel density in differentially "targeting" bAPs.

2 Methods

2.1 The model

The model had a soma with a diameter and length of 11.6 µm and a single 300 µm dendrite that had a diameter of 1.8 µm that branched into two 300 µm dendrites (Fig 1a). The daughter dendrites had the same diameter as each other, but the diameters were varied indirectly by varying the geometric ratio of the branch point from 0.1 to 2.0. The soma had the same conductances as [2] including the proximal form of the A-type potassium current. The dendrites used the same conductances as [2] except that only the distal form of the A-type potassium current was used and its concentration was constant within each main dendrite instead of following a gradient. The maximal conductance of the A-type potassium current ($\bar{g}_{Ka}$) was varied in one of the branch dendrites (referred to as the experimental branch, represented with red) while the other branch had a fixed $\bar{g}_{Ka}$ of 0.048 siemens / cm^2 (referred to as the constant branch, represented with blue). See Fig 1b for values of $\bar{g}_{Ka}$ in the experimental branch.

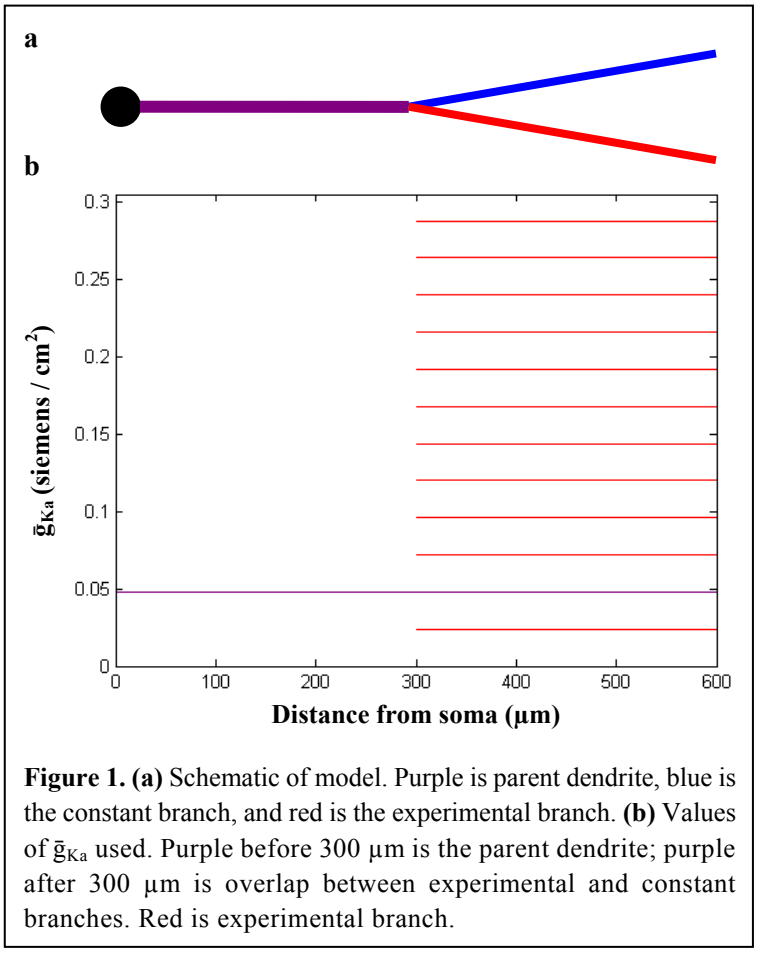

Figure 1. (a) Schematic of model. Purple is parent dendrite, blue is the constant branch, and red is the experimental branch. **(b)** Values of $\bar{g}_{Ka}$ used. Purple before 300 µm is the parent dendrite; purple after 300 µm is overlap between experimental and constant branches. Red is experimental branch.

Geometric ratio (GR) was calculated using the formula [6]:

$$GR = \frac{\sum_j d_j^{3/2}}{d_p^{3/2}}$$

Where d_p is the diameter of the parent dendrite, and d_j is the diameter of the j^{th} child dendrite.

A GR less than one produces a transient increase in action potential height, while a GR greater than one produces a transient decrease. A GR of one has no effect on action potential height [2].

2.2 Membrane dynamics modeling using Neuron

Neuron was used to model the membrane dynamics of the system. The script was made to save the peak voltage between the soma and the end of the two branches at every time point. If the overall peak lied before the branch, then it is the same for both paths, otherwise the peaks were at different locations. It is possible for one branch to have a peak voltage after the branch point and the other branch to have a peak before the branch point.

2.3 Traveling wave attractor using XPPAUT

In order to isolate the contribution of morphological and channel properties to the successful invasion of bAPs into the dendrite, we computed traveling wave attractors for each of the principal branches of the dendrite. As show previously (Hodgkin & Huxley, Acker & White), by assuming a traveling wave solution exists, we can find an underlying stable solution to the full biophysical membrane model. A traveling wave is found by analyzing the ODE model in XPPAUT. The model was adapted from that in ModelDB (accession number 118014). Parameters were managed in Matlab, then passed to XPPAUT for stable state analysis. The algorithm sought a value for K (which is proportional to wave speed) by trying different values and converging on the value which was closest to creating a stable solution. Once a stable solution is found, the amplitude of the peak and speed of the traveling wave attractor is stored. This is repeated for each combination of the range of diameter and $\bar{g}_{Ka}$.

3 Results

3.1 Membrane dynamics

The membrane dynamic simulations had back-propagating action potentials that were able to reach the terminal of the constant branch in all cases. As the bAP reached the terminal edge effects could be seen. Transient increase and decreases in bAP height were seen as expected with different GR values. Most cases could be easily seen as failures or successes, however there were a few cases where it was ambiguous. Two examples are shown in Figure 2.

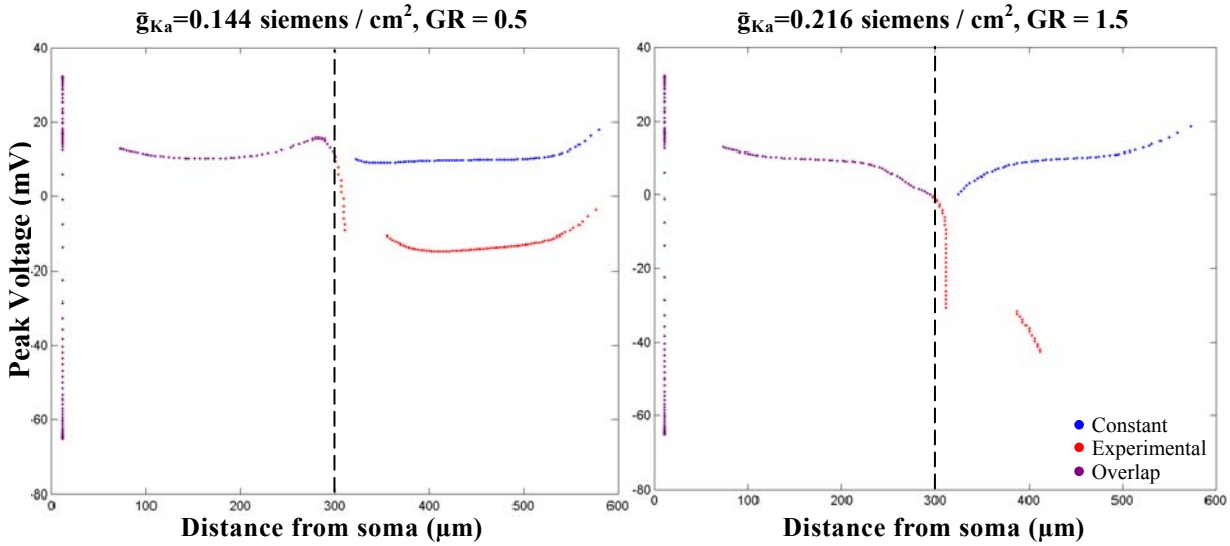

Figure 2. Example bAP peak for two sets of parameters. Dashed horizontal line indicates branch point. The left panel shows the bAP was successfully able to go the length of the dendrites while in the right panel the bAP failed. The left panel also shows the transient increase at the branch point due to GR<1 whereas the right panel shows a transient decrease for GR>1. Edge effects can be seen as the bAP reaches the end of the dendrite.

The peak voltage when the bAP was at 450 µm is shown in Figure 3 for the constant and experimental branches. A distance of 450 µm was selected as it was half-way down the branch reducing edge and initial branch effects. The constant branch had small variability in the peak voltage, from 9.7 mV to 10.7 mV. It varied mostly with changes in GR however it also varied slightly with changes in $\bar{g}_{Ka}$ for the experimental branch. The experimental branch showed two orders of magnitude greater variability of the peak voltage, ranging from -65 mV (the resting potential) to 45 mV. Most of the variability was due to the changes in $\bar{g}_{Ka}$ however there is slight variability in peak voltage with the change in GR. The largest effect of changes in GR is seen when $\bar{g}_{Ka}$ is equal to 0.192 siemens / cm^2. Inspection of the distance vs. peak voltage data (like in Figure 2) reveals that in these cases the peak voltage is slowly dropping towards the resting potential. The GR is simply prolonging the drop to resting potential but the bAP has failed active propagation.

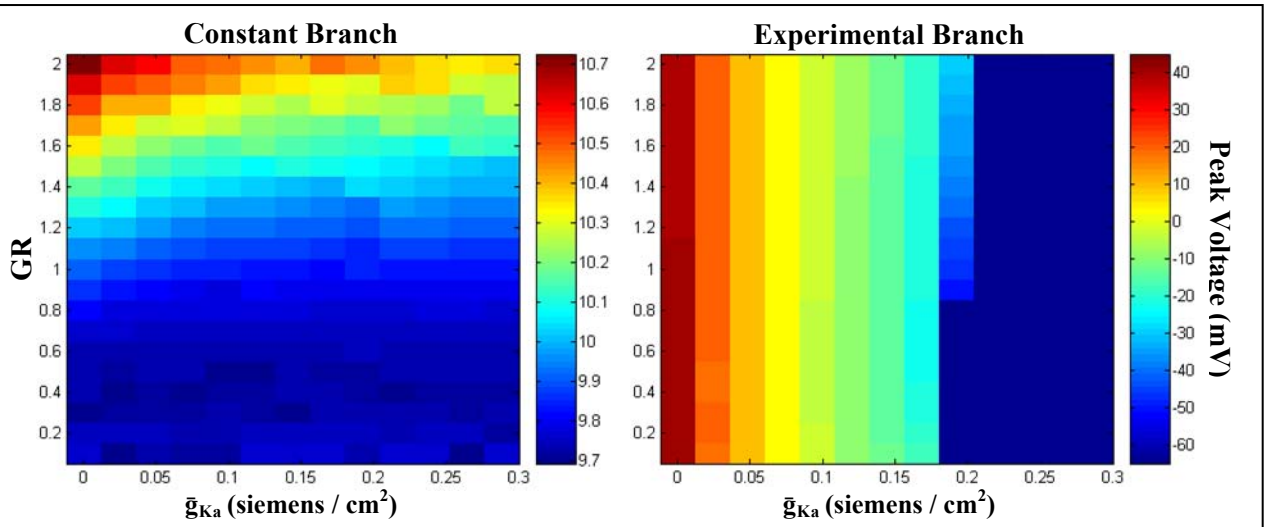

Figure 3. Peak voltage at 450 µm for the constant (left graph) and experimental (right graph) branches with varying GR and $\bar{g}_{Ka}$. The range of voltages for the constant branch is 1 mV while the range for voltages on the experimental branch is 110 mV. The resting potential of the cell is -65 mV.

The time that the bAP arrives at 450 µm is also affected by varying GR and $\bar{g}_{Ka}$ (Figure 4a). Arrival time is defined as the time relative to stimulation when the peak voltage along the branch is at 450 µm. The arrival times varied over GR and $\bar{g}_{Ka}$ of the experimental branch. GR had more influence for the control branch while both affected the experimental branch. As with peak voltage, the bAPs seen at 0.192 siemens / cm^2 were simply waves that were already failing and not actively propagating. The difference in arrival times (Figure 4b) shows that the bAPs for the different branches are moving at different speeds, with higher $\bar{g}_{Ka}$ or smaller GR causing larger delays in the experimental branch.

3.2 Travelling wave attractor

These rapid decreases in the peak amplitude of the bAPs could be predicted in the amplitude and failure of the underlying travelling wave. The peak amplitude of the travelling wave decreased with increasing $\bar{g}_{Ka}$ until the attractor state could no longer be maintained at 196 mS/cm^2 (Figure 5). Though this closely matches the results for the membrane dynamics, it is interesting to note that the diameter of the dendrite does not affect a change in the amplitude of the travelling wave. This implies that the modest peak which is maintained in the membrane dynamics at high geometric ratios is an indication of the system changing from the travelling wave state to a resting state.

Though the diameter of the dendrite does not have an effect on the amplitude of the travelling wave attractor, it has a direct effect on the speed of the travelling wave attractor. When estimating the timing delay between the arrival of the travelling wave attractors at 150um distal to the branch in each dendrite, we see that the timing greatly depends on the interaction between the A- type K+ currents and diameter of the dendrite. The trend is similar to that

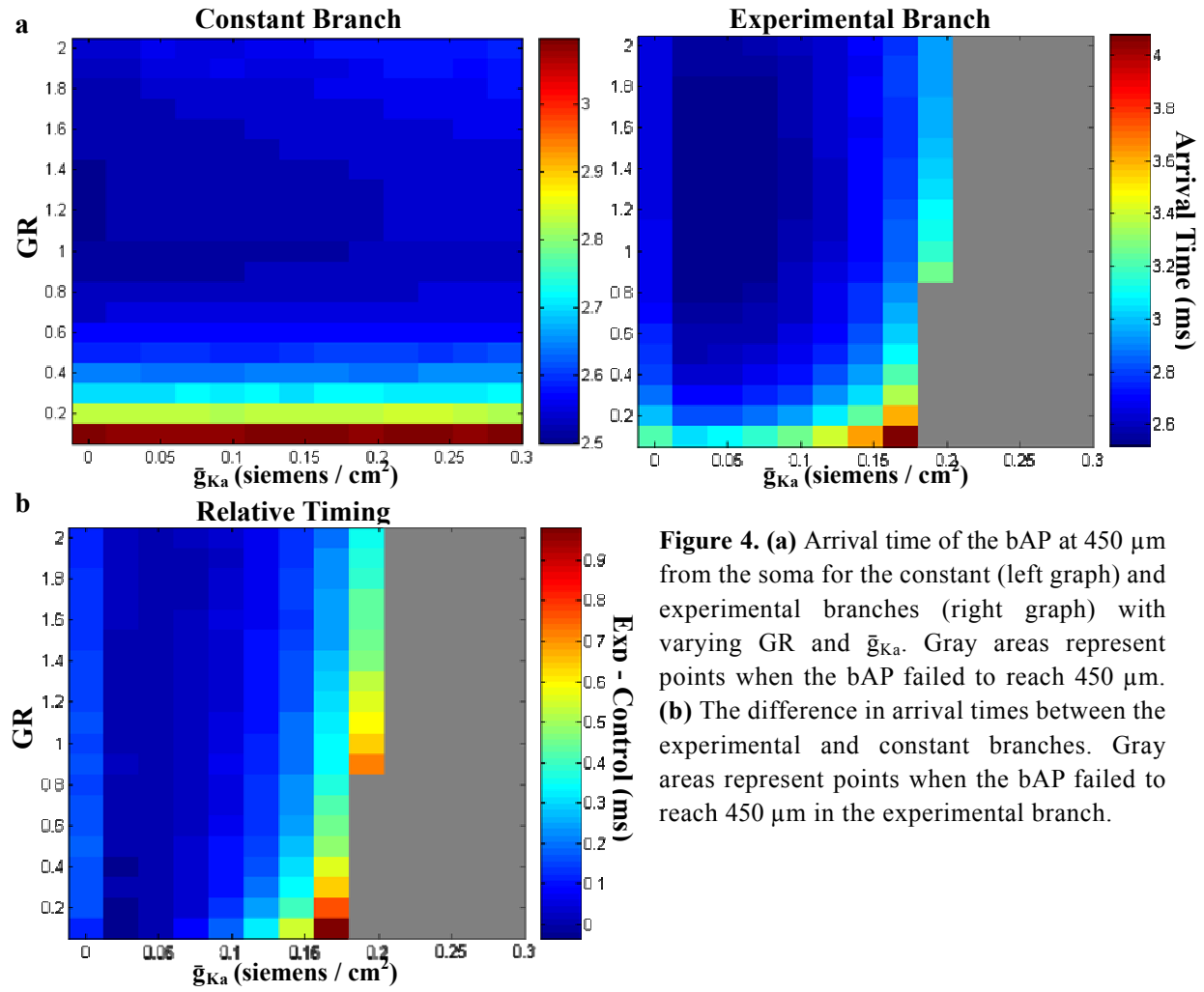

Figure 4. (a) Arrival time of the bAP at 450 µm from the soma for the constant (left graph) and experimental branches (right graph) with varying GR and $\bar{g}_{Ka}$. Gray areas represent points when the bAP failed to reach 450 µm. **(b)** The difference in arrival times between the experimental and constant branches. Gray areas represent points when the bAP failed to reach 450 µm in the experimental branch.

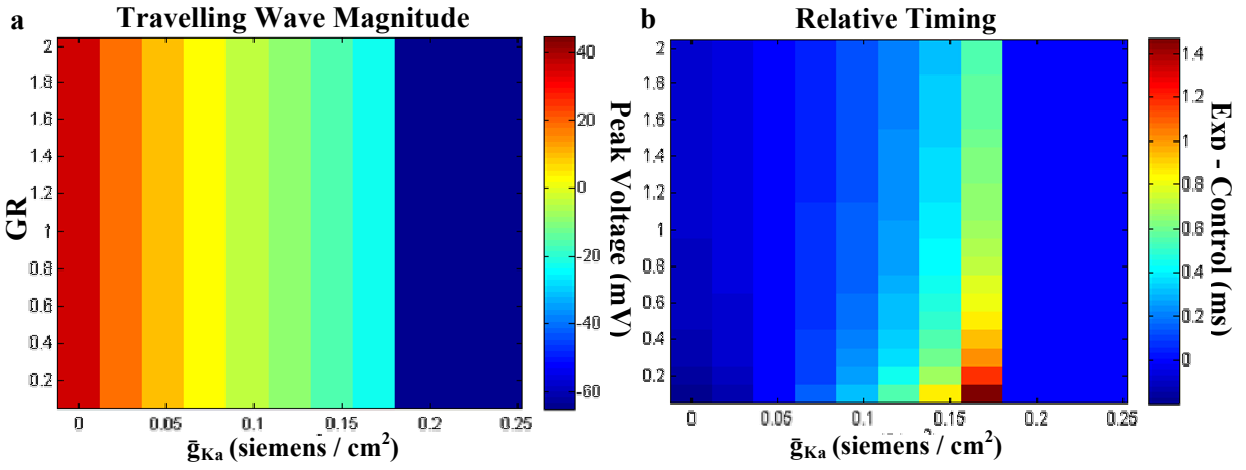

Figure 5. (a) Peak travelling wave amplitude at 450 µm for the experimental branch with varying GR and $\bar{g}_{Ka}$. **(b)** The relative timing between the two branches for varying GR and $\bar{g}_{Ka}$.

shown in the membrane dynamics (Figure 4b), however, the discrepancy in the values for these two measures are likely due to wave propagation changes at the branch point which are not accounted for in the travelling wave attractor.

4 Discussion

The two key components which can be modulated for STDP are the timing of the postsynaptic calcium influx relative to the excitatory post-synaptic potential and its magnitude. As the magnitude of calcium influx is largely dependent on the amplitude of the bAP, this model indicates that local increases in A-type K+ channel densities in select dendritic branches has significant potential to affect the strength of long term depression or potentiation. This variation in bAP amplitude is largely indifferent to changes in dendritic diameter. Though high values of $\bar{g}_{Ka}$ have more severe attenuation effects on smaller diameter dendrites, the lack of a change in the travelling wave attractor peak with changes in diameter indicates that the variation is due to deviations from the travelling wave attractor.

Though diameter differences do not have an effect on bAP amplitudes, they do affect the wave speed. This is seen both in the simulation and in the travelling wave attractor. It is important to note that the differences seen in the relative timing of the bAPs is due exclusively to the increased $\bar{g}_{Ka}$ on the experimental branch, as the experimental and control branches have the same diameter. As the most severe time lags in our model (around 1ms) are seen in small branches, this indicates that, for a given range of possible $\bar{g}_{Ka}$ values, timing will vary the most in small branches.

The two methods each showed different things that the other method did not. The membrane dynamics was modeling what actually would in the system and neighboring locations have effects on each other. For example, change in $\bar{g}_{Ka}$ of one branch effect the peak voltage of the bAP in the other branch, or a branch point causes a transient change in the peak voltage. Even though the traveling wave attractor is unable to say anything about interactions of this nature it is a much better predictor of whether or not the bAP is being actively propagated, especially in the edge cases when the currents are slowly dying out.

It may be useful to explore focal changes in A-type K+ channel densities at branch points. The current model results in scaled amplitude and timing changes, but focal changes at branch points could completely block bAPs. Also, as this model seems to be important for STDP, it may be useful to integrate these changes in an STDP model in order to assess the functional changes incurred by the amplitude and timing modulations seen here.

Acknowledgments

We would like to thank Gert Cauwenberghs, Chris MacDonald, Doug Rubino, and our classmates in the BGGN 260 Neurodynamics class for their helpful feedback on this project.

References

[1] Spruston et al. (1995) Activity-dependent action potential invasion and calcium influx into hippocampal CA1 dendrites. *Science* **268**(5208):297-300.

[2] Acker and White. (2007) Roles of IA and morphology in action potential propagation in CA1 pyramidal cell dendrites. *Journal of computational neuroscience* **23**(2):201-16.

[3] Chen et al. (2006) Deletion of Kv4.2 gene eliminates dendritic A-type K+ current and enhances induction of long-term potentiation in hippocampal CA1 pyramidal neurons. *J Neurosci* **26**(47):12143-51.

[4] Kim et al. (2007) Regulation of dendritic excitability by activity-dependent trafficking of the A-type K+ channel subunit Kv4.2 in hippocampal neurons. *Neuron* **54**(6):933-47.

[5] Makara et al. (2009) Experience-dependent compartmentalized dendritic plasticity in rat hippocampal CA1 pyramidal neurons. *Nat Neurosci* **12**(12):1485-7.

[6] Rall, W. (1959). Branching dendritic trees and motoneuron membrane resistivity. Experimental Neurology, 1, 491–527.